On-Line Inference of Polymer Properties in an Industrial Polyethylene Reactor

K. B. McAuley and J. F. MacGregor
Dept. of Chemical Engineering, McMaster University, Hamilton, Ontario, Canada L8S 4L7

A major difficulty affecting the control of product quality in industrial polymerization reactors is the lack of suitable on-line polymer property measurements. In this article a scheme is developed to predict melt index and density in a fluidized-bed ethylene copolymerization reactor. Theoretically-based models are derived to predict quality variables from the available on-line temperature and gas composition measurements. Adjustable parameters in these models are updated on-line using infrequent laboratory measurements and a recursive parameter estimation technique. The application of this methodology is illustrated using operating data from an industrial reactor. It is shown that both melt index and density can be successfully predicted. Knowledge of product property deviations from desired targets is required so that manufacturers can take corrective actions to reduce the quantity of off-grade material made and produce a consistent product.

Introduction

A common problem in the polymer industry is the lack of on-line measurement technology for polymer quality variables (Elicabe and Meira, 1988; MacGregor et al., 1984). While temperature, pressure, flow rate and gas composition are routinely measured on-line, key quality variables such as molecular weight and copolymer composition must usually be measured off-line in quality control laboratories (Richards and Schnelle, 1988). These delayed and infrequent quality measurements provide essential feedback for process control. Combination of information from on-line and off-line measurements with process models can lead to improved estimates of quality variables between samples and to improved product property control. Reconciliation of measurement information with process models can be accomplished in several ways. Recursive parameter estimation techniques (Ljung, 1987) can be used to update model parameters. Alternatively, Kalman filters (Ardell and Gumowski, 1983; Kozub and MacGregor, 1989; MacGregor et al., 1986; Ellis et al., 1988) can be used to infer unmeasured product quality states as well as to update model parameters and model predictions.

In this article, a scheme to infer polymer quality variables in a fluidized-bed polyethylene reactor is presented. A brief process description is followed by the development of theoretically-based models relating reactor operating conditions to molecular weight and copolymer composition. In industrial settings, polyethylene-grade specifications are generally quoted in terms of melt index (MI) and density (ρ) (ASTM, 1990), rather than molecular weight and comonomer content. Hence, relationships between molecular weight and MI and between composition and ρ have been incorporated into the process models. The development of a recursive technique for updating model parameters using off-line MI-and ρ measurements is described. Results show that both MI and ρ can be successfully predicted using this technique. Although the inference technique presented is discussed in the context of predicting melt index and density in gas-phase polyethylene reactors, the approach is applicable to other chain growth polymerization systems with well-defined reactor mixing behavior.

Correspondence concerning this article should be addressed to J. F. MacGregor.

Process Description

In recent years, the UNIPOL process has become a popular commercial technology for linear polyethylene production (Burdett, 1988). In this process, the copolymerization of ethylene and α-olefins is carried out in a fluidized-bed reactor using a heterogeneous Ziegler-Natta or supported metal oxide catalyst. A schematic diagram of the reactor system is shown in Figure 1. The feed to the reactor comprises ethylene, a

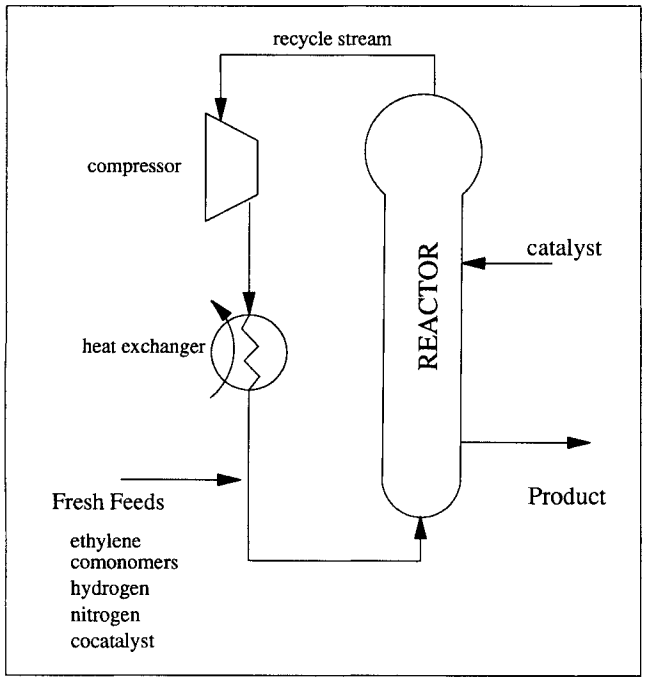

Figure 1. Gas-phase polyethylene reactor system.

comonomer (1-butene or a higher alpha-olefin) hydrogen and nitrogen. These gases provide the fluidization and heat transfer media and supply reactants for the growing polymer particles. The catalyst and a cocatalyst are fed continuously to the reactor. The fluidized particles disengage from the reactant gas in the expanded top section of the reactor. The unreacted gases are combined with fresh feed streams and recycled to the base of the reactor. Since the reaction is highly exothermic, heat must be removed from the recycle gas before it is returned to the reactor. The rate of polymer production is determined from an on-line heat balance. The mass of material in the bed is also calculated on-line using bed level and pressure measurements. The conversion per pass through the bed is very low, making the recycle stream much larger than the fresh feed streams. Because polymer particles in the fluidized bed are mixed well and the conversion per pass is low, gas composition and temperature are essentially uniform throughout the bed. Periodically, the product discharge valve near the base of the reactor opens and the fluidized product flows into a surge tank. The unreacted gas is recovered from the product that proceeds downstream for further processing and distribution.

The melt index and density of the polymer in the bed depend on catalyst properties, reactant gas composition, and reactor temperature. The reactor is instrumented well with temperature, pressure, and flow sensors. Gas compositions are measured by on-line gas chromatographs. Melt index and density are measured every several hours in the quality control laboratory. These analyses require up to one hour. When the lab results become available, they are used to adjust the reactor operating conditions to ensure that on-specification polymer is produced.

Models for Melt Index and Density

Any scheme to predict melt index and density between measurements requires a model describing how these variables are affected by reactor operating conditions. If the reactor is operated near one set of operating conditions to produce a limited number of polymer products, then an empirical linear plant model will often suffice. However, one of the advantages of the UNIPOL process over traditional liquid-phase systems is the wider range of products that can be produced (Burdett, 1988). The models developed for this application must be valid over the range of products made in the reactor. Thus, linear empirical models are not suitable.

A kinetic model describing molecular weight and copolymer composition development and their relationships to melt index and density is presented by McAuley et al. (1990). While this model can predict *MI*, ρ, and production rate in an industrial reactor, the structure of this model (22 differential equations) is prohibitively complex for use in an on-line quality inference scheme. The approach taken in this article is to simplify the theoretical model so that it becomes appropriate for on-line use. Although several different comonomers are used to produce linear polyethylene in UNIPOL systems, it is uncommon to operate with ethylene and more than two comonomers in the reactor simultaneously. Hence, the simple models for *MI* and ρ are developed for ethylene, butene and one higher alpha-olefin (HAO) comonomer. Extensions to more comonomers are straightforward.

Unmeasured impurities and unmodeled disturbances can result in sustained offset between model predictions and measured quality variables. If such drifts in product quality are not accounted for in the control scheme, then large quantities of off-grade polymer can be produced. One way to alleviate this problem is to force the model to track the process by updating parameters and predictions recursively on-line. If the common sources of the expected mismatch are known, then this information can be used to choose which parameters remain constant and which are likely to change due to the disturbances. Theoretically-based models have an advantage over empirical models in that the designer may have some prior knowledge about which parameters require on-line updating. Usually only a few meaningful parameters need to be updated, thereby making the on-line schemes easier to maintain and monitor.

Instantaneous vs. cumulative properties

Polymerization reactions involving Ziegler-Natta catalysts occur very quickly compared with the time scale of the gas-phase and solid-phase reactor dynamics. Under the assumption of uniform gas composition and temperature, all of the polymer made during a short time interval at a specific type of catalyst site is similar in structure because it is produced under the same reaction conditions. The composition and molecular weight distributions of the polymer produced during this short time period are referred to as instantaneous properties, whereas the molecular weight and composition distributions of the total polymer in the fluidized bed are cumulative properties. At steady state, the instantaneous and cumulative properties are identical. However, under unsteady conditions, instantaneous and cumulative properties can be significantly different. Cumulative polymer properties can be obtained by integrating the contributions of instantaneous polymer produced in the past, as is done in this application. First, models are developed for instantaneous melt index and density, and then a dynamic mass balance on the fluidized bed is used to obtain the cumulative properties.

Instantaneous melt index model development

Above a certain critical molecular weight, the viscosity, η, of a linear polymer melt at low shear rates is related to the weight average molecular weight, $\overline{M}_w$, by:

$$\eta \propto \overline{M}_w^{\,a} \tag{1}$$

where the exponent a is approximately 3.5 (Vinodograv and Malkin, 1980). Since melt index is inversely proportional to the low shear viscosity, MI and $\overline{M}_w$ are related by:

$$MI \propto \overline{M}_w^{\,-3.5} \tag{2}$$

This power law relationship has been confirmed experimentally for linear polyethylenes by Bremner et al. (1990).

Gas-phase Ziegler-Natta olefin copolymerizations are generally controlled by reaction kinetics rather than by monomer diffusion limitations (Floyd et al., 1986). The broad molecular weight and compositional distributions that have been observed for these systems (Usami et al., 1986) result from multiple types of active sites on the catalyst. The polymer produced at each individual site type contributes to the overall product properties. In this system, growing polymer chains are terminated exclusively by chain transfer and site deactivation reactions. The instantaneous molecular weight distribution for polymer made at each site type is the Flory-Schultz most probable distribution and the corresponding polydispersity is 2 (Rudin, 1989). Thus, for an active site of type j, the instantaneous $\overline{M}_w$ and number average molecular weight, $\overline{M}_n$, are related by:

$$\overline{M}_w(j) = 2\overline{M}_n(j) \tag{3}$$

Hence, the instantaneous MI of the polymer produced at a site of type j is related to $r_n(j)$, the instantaneous number average degree of polymerization by:

$$MI(j) \propto \left[\frac{1}{r_n(j)}\right]^{3.5} \tag{4}$$

$r_n(j)$ is equal to the ratio of the rate of propagation of living polymer chains, $R_p(j)$, to the rate of production of dead chains, $R_{tr}(j)$:

$$r_n(j) = \frac{R_p(j)}{R_{tr}(j)} \tag{5}$$

$R_p(j)$ is the sum of the consumption rates for individual monomers:

$$R_p(j) = R_{p1}(j) + R_{p3}(j) \tag{6}$$

$$R_{p1}(j) = [M_1]\{kp_{11}(j)\phi_1(j) + kp_{21}(j)\phi_2(j) + kp_{31}(j)\phi_3(j)\}C^*(j) \tag{7}$$

$$R_{p2}(j) = [M_2]\{kp_{12}(j)\phi_1(j) + kp_{22}(j)\phi_2(j) + kp_{32}(j)\phi_3(j)\}C^*(j) \tag{8}$$

$$R_{p3}(j) = [M_3]\{kp_{13}(j)\phi_1(j) + kp_{23}(j)\phi_2(j) + \mathrm{kp}_{33}(\mathrm{j})\phi_3(\mathrm{j})\}\mathrm{C}^*(\mathrm{j}) \tag{9}$$

The individual propagation rates depend on $[M_1]$, $[M_2]$ and $[M_3]$, which are the concentrations ethylene, butene and HAO in the gas phase, and on $C^*(j)$, the number of moles of active sites of type j in the reactor. The $kp_{im}(j)$ terms are propagation rate constants for the addition of monomer m to a growing chain with terminal monomer i. $\phi_i(j)$ is the fraction of propagating sites of type j, which have terminal monomer i. Expressions for $\phi_1(j)$, $\phi_2(j)$ and $\phi_3(j)$ are discussed by McAuley (1990).

For industrial polyethylenes, the incorporation of comonomer into the polymer chains is generally less than 5 mole per cent (Sinclair, 1983). Thus, at any one time, the fraction of growing chains with a terminal butene or HAO group is expected to be small. Propagation rate constants for the addition of a given monomer to the chain are of the same order of magnitude, regardless of the terminal monomer on the growing chain. As a result, the first term in the parentheses in Eq. 7 is much larger than the remaining two terms. Similarly, the first terms in Eqs. 8 and 9 are much larger than the terms that follow them. Substitution into Eq. 6 with the added assumption that $\phi_1(j)$ is near unity gives:

$$R_p(j) = \{[M_1]kp_{11}(j) + [M_2]kp_{12}(j) + [M_3]kp_{13}\}C^*(j) \tag{10}$$

Neglecting spontaneous transfer and deactivation reactions, the rate of production of dead chains consists of transfer to monomer, transfer to hydrogen, transfer to cocatalyst and impurity deactivation terms:

$$R_{tr}(j) = R_{f1}(j) + R_{f2}(j) + R_{f3} + R_{fH}(j) + R_{fR}(j) + R_{dI}(j) \tag{11}$$

The rates of chain transfer to ethylene, butene, HAO, hydrogen and cocatalyst are shown below:

$$R_{f1}(j) = [M_1]\{kf_{11}(j)\phi_1(j) + kf_{21}(j)\phi_2(j) + \mathrm{kf}_{31}(\mathrm{j})\phi_3(\mathrm{j})\}\mathrm{C}^*(\mathrm{j}) \tag{12}$$

$$R_{f2}(j) = [M_2]\{kf_{12}(j)\phi_1(j) + kf_{22}(j)\phi_2(j) + \mathrm{kf}_{32}(\mathrm{j})\phi_3(\mathrm{j})\}\mathrm{C}^*(\mathrm{j}) \tag{13}$$

$$R_{f3}(j) = [M_3]\{kf_{13}(j)\phi_1(j) + kf_{23}(j)\phi_2(j) + \mathrm{kf}_{33}(\mathrm{j})\phi_3(\mathrm{j})\}\mathrm{C}^*(\mathrm{j}) \tag{14}$$

$$R_{fH}(j) = [\mathrm{H_2}]\{kf_{1\mathrm{H}}(j)\phi_1(j) + kf_{2\mathrm{H}}(j)\phi_2(j) + \mathrm{kf}_{3\mathrm{H}}(j)\phi_3(j)\}C^*(j) \tag{15}$$

$$R_{fR}(j) = [R]\{kf_{1R}(j)\phi_1(j) + kf_{2R}(j)\phi_2(j) + \mathrm{kf}_{3R}(j)\phi_3(j)\}C^*(j) \tag{16}$$

$[\mathrm{H_2}]$ and $[R]$ are the concentrations of hydrogen and cocatalyst, respectively. The kf's are transfer rate constants defined by McAuley (1990). The rate of active site deactivation by impurities, $R_{dI}(j)$, is:

$$R_{dI}(j) = [I]kdI(j)C^*(j) \quad (17)$$

$[I]$ is the concentration of impurities in the reactor and $k_{dI}(j)$ is a deactivation rate constant. Equations 12 to 16 can be simplified in a similar manner to Eqs. 7 to 9. Equations 10 to 17 can then be combined to give the following expression:

$$\frac{R_{tr}(j)}{R_p(j)} = \frac{[M_1]kf_{11}(j) + [M_2]kf_{12}(j) + [M_3]kf_{13}(j) + [H_2]kf_{1H}(j) + [R]kf_{1R}(j) + [I]kdI(j)}{[M_1]kp_{11}(j) + [M_2]kp_{12}(j) + [M_3]kp_{13}(j)} \quad (18)$$

This equation can be further simplified by neglecting $[M_2]kp_{12}(j)$ and $[M_3]kp_{13}(j)$ in the denominator. This can be done without incurring much additional error because the incorporation of butene and HAO into the polymer chains is small compared with ethylene incorporation. Combination of Eqs. 5 and 18 yields:

$$\frac{1}{r_n(j)} = \frac{kf_{11}(j)}{kp_{11}(j)} + \frac{kf_{12}(j)[M_2]}{kp_{11}(j)[M_1]} + \frac{kf_{13}(j)[M_3]}{kp_{11}(j)[M_1]} + \frac{kf_{1H}(j)[H_2]}{kp_{11}(j)[M_1]} + \frac{kf_{1R}(j)[R]}{kp_{11}(j)[M_1]} + \frac{kdI(j)[I]}{kp_{11}(j)[M_1]} \quad (19)$$

resulting in the following relationship between melt index and the reaction kinetics:

$$MI(j) \propto \left\{ \frac{kf_{11}}{kp_{11}} + \frac{kf_{12}[M_2]}{kp_{11}[M_1]} + \frac{kf_{13}[M_3]}{kp_{11}[M_1]} + \frac{kfh_1[H_2]}{kp_{11}[M_1]} + \frac{kfr_1[R]}{kp_{11}[M_1]} + \frac{kdI[I]}{kp_{11}[M_1]} \right\}^{3.5} \quad (20)$$

The j's on the righthand side of Eq. 20 have been eliminated in the interest of brevity. The effect of temperature on melt index can be incorporated into the model by assuming that all chain transfer and deactivation reactions have a similar activation energy, Ea_{tr}. For a general chain transfer rate constant, $kf(T)$, Arrhenius behavior implies that:

$$kf(T) = kf(T_0)\exp\left(-\frac{Ea_{tr}}{R}\left\{ \frac{1}{T} - \frac{1}{T_0} \right\} \right) \quad (21)$$

where T_0 is a reference temperature. Thus, the ratio of a chain transfer rate constant to kp_{11} is:

$$\frac{kf(T)}{kp_{11}(T)} = \frac{kf(T_0)}{kp_{11}(T_0)} \exp\left(\frac{-Ea_{tr} + Ea_p}{R}\left\{ \frac{1}{T} - \frac{1}{T_0} \right\} \right) \quad (22)$$

where Ea_p is the activation energy for propagation. Equation (20) becomes:

$$MI(j) = \exp\left\{ k_7\left(\frac{1}{T} - \frac{1}{T_0} \right) \right\} \left\{ k_6 + k_1\frac{[M_2]}{[M_1]} + k_2\frac{[M_3]}{[M_1]} + k_3\frac{[H_2]}{[M_1]} + k_4\frac{[R]}{[M_1]} + k_5\frac{[I]}{[M_1]} \right\}^{3.5} \quad (23)$$

The overall instantaneous melt index of the polymer could be calculated from the individual, site-specific, instantaneous melt indices, $MI(1)$ and $MI(2)$, if the parameters in Eq. 23 were known for each site type. The overall instantaneous weight average molecular weight of the combined polymer produced at two different active site types is:

$$\overline{M}_w = w_1\overline{M}w(1) + w_2\overline{M}_w(2) \quad (24)$$

where w_1 and w_2 are the weight fractions of the polymer produced at sites 1 and 2, and $\overline{M}_w(1)$ and $\overline{M}_w(2)$ are the corresponding weight average molecular weights. From Eq. 2:

$$MI^{-0.286} = w_1MI(1)^{-0.286} + w_2MI(2)^{-0.286} \quad (25)$$

Since it is very difficult to determine, the parameters k_1 to k_7 for each separate active site type, it is proposed that the same structure as Eq. 23 be used to predict the overall instantaneous melt index. The parameters values k_1 to k_7 will be influenced by the combined effects of the individual sites. When catalyst-grade changes are made, altering the ratio of the two types of sites, the values of the parameters will change. Taking natural logarithms of both sides of Eq. 23 and eliminating the j gives the final model form:

$$\ln(MI) = k_7\left(\frac{1}{T} - \frac{1}{T_0} \right) + 3.5\ln\left(k_6 + k_1\frac{[M_2]}{[M_1]} + k_2\frac{[M_3]}{[M_1]} + k_3\frac{[H_2]}{[M_1]} + k_4\frac{[R]}{[M_1]} + k_5\frac{[I]}{[M_1]} \right) \quad (26)$$

Although many assumptions and simplifications have been made to obtain this instantaneous MI model, the main mechanisms that affect molecular weight development are still reflected in the model structure.

Instantaneous density model development

The density of a polymer sample depends on how closely the polymer chains can fit together. Incorporation of comonomers into polyethylene causes short chain branches (SCB's) to protrude from the polymer backbone. These SCB's inhibit crystalline structures and reduce the density of the polymer. Both the number of branches along the chain and the length of the side chains influence density. Polymer molecular weight or alternatively melt index also has a small influence on polyethylene density (Sinclair, 1983). A model of the form:

$$\rho = p_0 + p_1\ln(MI) - \{a_2mf_2 + a_3mf_3\}^{p_4} \quad (27)$$

reflects these ideas. mf_2 and mf_3 are the mole fractions of butene and HAO, respectively, in the polymer chains. As mf_2 and mf_3 increase, the number of SCB's increases causing the density to fall. Parameters a_2 and a_3 differ because the side chains produced by the HAO are longer than those produced

by butene. A smaller mole fraction of HAO than butene is required to produce the same drop in density. When ethylene homopolymer is produced, mf_2 and mf_3 are zero. Thus, p_0 represents the density of pure homopolymer with a melt index of unity.

At a site of type j, the instantaneous mole fraction of butene in the polymer chain is:

$$mf_2(j) = \frac{R_{p2}(j)}{R_p(j)} \tag{28}$$

When comonomer incorporation is small, this expression reduces to:

$$mf_2(j) = \frac{[M_2]kp_{12}(j)}{[M_1]kp_{11}(j)} \tag{29}$$

Similarly for the HAO:

$$mf_3(j) = \frac{[M_3]kp_{13}(j)}{[M_1]kp_{11}(j)} \tag{30}$$

The overall mole fraction of butene and HAO in the polymer depends on the relative numbers of the two active site types:

$$mf_2 = m_1 mf_2(1) + m_2 mf_2(2) \tag{31}$$

$$mf_3 = m_1 mf_3(1) + m_2 mf_3(2) \tag{32}$$

where m_1 and m_2 are the mole fractions of the total monomer being consumed instantaneously at site types 1 and 2, respectively. Thus, for a given catalyst:

$$mf_2 \propto \frac{[M_2]}{[M_1]} \tag{33}$$

$$mf_3 \propto \frac{[M_3]}{[M_1]} \tag{34}$$

The instantaneous density model becomes:

$$\rho = p_0 + p_1 \ln(MI) - \left\{ p_2 \frac{[M_2]}{[M_1]} + p_3 \frac{[M_3]}{[M_1]} \right\}^{p_4} \tag{35}$$

The structure of this model agrees with the observation that reactor temperature has a minimal effect on the density of polyethylene. Temperature effects enter the preceding model only through the melt index term.

Cumulative melt index and density models

When two polymer samples, labeled A and B, with different molecular weights are mixed together, $\overline{M}_w$ of the mixture is given by:

$$\overline{M}_w = w_A \overline{M}_{wA} + w_B \overline{M}_{wB} \tag{36}$$

where w_A and w_B are the weight fractions of polymers A and B in the mixture and $\overline{M}_{wA}$ and $\overline{M}_{wB}$ are the respective weight average molecular weights. If the same samples have densities ρ_A and ρ_B and no volume change occurs during the mixing process, then the overall density is given by:

$$\frac{1}{\rho} = \frac{w_A}{\rho_A} + \frac{w_B}{\rho_B} \tag{37}$$

In UNIPOL reactors, the solid polymer particle phase is mixed well by the turbulent action of the gas phase. New polymer is added continuously to the bed by the polymerization of monomers, and the accumulated polymer leaves the bed in frequent small batches via the product discharge system. Hence, the mixing and residence time behavior of the solid phase can be approximated by that of an ideal continuous stirred tank. Instantaneous polymer with weight average molecular weight $\overline{M}_{wi}$, melt index MI_i, and density ρ_i is fed continuously to the mixer at a mass flow rate P_R equal to the instantaneous polymer production rate. The well-mixed bed contains a mass of polymer, M_p, which has a cumulative weight average molecular weight $\overline{M}_{wc}$, cumulative melt index MI_c, and cumulative density ρ_c. If there is no net accumulation of polymer during a short period of time, Δt, then $P_R \Delta t$ kg of new instantaneous polymer enter the bed and the same quantity of cumulative polymer leaves the bed. After the time period, Δt, the mass fraction of new instantaneous polymer in the reactor will be $P_R \Delta t / M_p$ and the mass fraction of the old cumulative polymer will be $1 - P_R \Delta t / M_p$. Thus, the new weight average molecular weight and density are given by:

$$\overline{M}_{wc}(t+\Delta t) = \frac{P_R \Delta t}{M_p} \overline{M}_{wi}(t) + \left(1 - \frac{P_R \Delta t}{M_p}\right) \overline{M}_{wc}(t) \tag{38}$$

$$\frac{1}{\rho_c(t+\Delta t)} = \frac{P_R \Delta t}{M_p} \frac{1}{\rho_i(t)} + \left(1 - \frac{P_R \Delta t}{M_p}\right) \frac{1}{\rho_c(t)} \tag{39}$$

Therefore,

$$\frac{\overline{M}_{wc}(t+\Delta t) - \overline{M}_{wc}(t)}{\Delta t} = \frac{1}{\tau} \overline{M}_{wi}(t) - \frac{1}{\tau} \overline{M}_{wc}(t) \tag{40}$$

$$\frac{\dfrac{1}{\rho_c(t+\Delta t)} - \dfrac{1}{\rho_c(t)}}{\Delta t} = \frac{1}{\tau} \frac{1}{\rho_i(t)} - \frac{1}{\tau} \frac{1}{\rho_c(t)} \tag{41}$$

where $\tau = M_p / P_R$ is the solid-phase residence time. Taking the limit as $\Delta t \to 0$ gives the following differential equations:

$$\frac{d\overline{M}_{wc}}{dt} = \frac{1}{\tau} \overline{M}_{wi} - \frac{1}{\tau} \overline{M}_{wc} \tag{42}$$

$$\frac{d\left(\dfrac{1}{\rho_c}\right)}{dt} = \frac{1}{\tau} \frac{1}{\rho_i} - \frac{1}{\tau} \frac{1}{\rho_c} \tag{43}$$

Equation 2 can be used to express Eq. 42 in terms of melt index:

$$\frac{d(MI_c^{-0.286})}{dt} = \frac{1}{\tau} MI_i^{-0.286} - \frac{1}{\tau} MI_c^{-0.286} \tag{44}$$

Given the initial cumulative MI and ρ of the polymer bed, Eqs. 43 and 44 can be used to predict the effects of time varying instantaneous MI and ρ on the cumulative properties. These cumulative properties are measured in the quality control laboratory.

Gas compositions in the reactor are measured periodically using on-line gas chromatographs. Since the gas sampling interval, h, is very small with respect to the polymer-phase residence time, τ, little error is incurred by assuming that the instantaneous properties remain constant over the gas sampling interval. Using this assumption, Eq. 44 is equivalent to the following difference equation:

$$MI_c^{-0.286}(t) = \exp(-h/\tau) MI_c^{-0.286}(t-h) + \{1-\exp(-h/\tau)\} MI_i^{-0.286}(t-h) \tag{45}$$

Similarly for density, Eq. 43 becomes:

$$\frac{1}{\rho_c(t)} = \exp(-h/\tau) \frac{1}{\rho_c(t-h)} + \{1-\exp(-h/\tau)\} \frac{1}{\rho_i(t-h)} \tag{46}$$

These are the model forms used in the on-line inference scheme. All that is required to predict cumulative melt index and density estimates are initial estimates of MI_c and ρ_c, estimates of the parameters $\underline{k} = (k_1, k_2, \ldots k_7)^T$ and $\underline{p} = (p_0, p_1, \ldots p_4)^T$ in the instantaneous property Eqs. 26 and 35, and a series of gas composition, temperature, production rate and bed mass measurements.

Recursive Techniques for Updating Parameters and Predictions in Nonlinear Models

Recursive techniques are ideal for updating model parameters in on-line applications. The traditional nonlinear least squares approach to parameter estimation is not used usually because it requires the storage of past input variables and observations in a table. As this data table continues to grow, successive calculations take longer to complete. In recursive schemes, the measured input and output data are processed sequentially and old measurements need not be stored. Each parameter updating step requires the same amount of computational effort. The approaches that can be used for recursive parameter estimation with nonlinear models include the extended Kalman filter and recursive prediction error methods (Ljung, 1987).

Extended Kalman filter

The extended Kalman filter (EKF) provides a framework for both state estimation and parameter updating in nonlinear process models. One of the first reported applications of this technique to polymer reactors was by Jo and Bankhoff (1976) who used an EKF to both estimate process states and update several time varying parameters on-line. Recent applications of EKF's to polymerization systems have been reported by Kozub and MacGregor (1989), by Gagnon (1990), and by Ellis et al. (1988) among others.

For the polyethylene reactor study in this article, the EKF could be implemented as follows. Given an initial set of parameter estimates $(\underline{k}^o, \underline{p}^o)$, and some initial estimate of the model states $(MI_c^{-0.286\,o}, 1/\rho_c^o)$, the nonlinear model Eqs. 45 and 46 can be linearized about these initial conditions to give:

$$\underline{x}(t) = \underline{A}(t)\underline{x}(t-1) + \underline{G}(t)\underline{u}(t) + \underline{w}(t) \tag{47}$$

$$\underline{y}(t) = \underline{H}(t)\underline{x}(t) + \underline{v}(t) \tag{48}$$

where $t-1$ refers to the time at which the last polymer sample was taken and t is the time of the current sample. The state vector $\underline{x}$ is an augmented vector consisting of the model and parameter states, that is:

$$\underline{x}^T = (MI_c^{-0.286}, 1/\rho_c, \underline{k}^T, \underline{p}^T) \tag{49}$$

The $\underline{A}$ and $\underline{G}$ matrices in Eq. 47 are composed of several parts as shown below:

$$\underline{A} = \left(\begin{array}{c|c} \underline{A}' & \underline{O} \\ \hline \underline{O} & \underline{I} \end{array}\right) \tag{50}$$

$$\underline{G}(t) = \begin{pmatrix} \underline{G}' \\ \hline \underline{O} \end{pmatrix} \tag{51}$$

The $\underline{A}'$ part in Eq. 49 is the linearized relationship describing how $MI_c^{-0.286}$ and $1/\rho_c$ at time $t-1$ contribute to the properties at time t. An expression for $MI_c^{-0.286}$ at time t can be obtained by successive application of Eq. 45 for each interval of length h contained in the product sampling interval from time $t-1$ to t. In a similar manner, $1/\rho_c$ can be determined by successive applications of Eq. 46. These equations can be linearized using Taylor series approximations to give $\underline{A}'$ and also $\underline{G}'$ in Eqs. 50 and 51. $\underline{y}(t)$ in Eq. 48 is the vector of new measurements available at time t and $\underline{H}(t) = (1, 0, \underline{0})$, $(0, 1, \underline{0})$ or $(1, 0, \underline{0})$ depending on which measurements are available at the current sampling interval. $\underline{u}$ is the set of inputs to the model including temperature and gas composition ratios. $\underline{w}$ and $\underline{v}$ represent the modeling errors and the measurement errors, with covariance matrices $\underline{R}_w$ and $\underline{R}_v$, respectively. When new measurements become available, the state estimation and parameter updating are accomplished by solving the following filter equation:

$$\underline{\hat{x}}(t \mid t) = \underline{\hat{x}}(t \mid t-1) + \underline{K}(t)\{\underline{y}(t) - \underline{\hat{y}}(t \mid t-1)\} \tag{52}$$

where $\underline{\hat{y}}(t \mid t-1)$ is the predicted output vector at time t made by evaluating the nonlinear model Eqs. 45 and 46 from time $t-1$ to t. The Kalman gain matrix $\underline{K}(t)$ comes from solving the following set of recursive matrix Ricatti equations:

$$\underline{K}(t) = \underline{P}(t \mid t-1)\underline{H}^T(t)[\underline{H}(t)\underline{P}(t \mid t-1) \times \underline{H}^T(t) + \underline{R}_v]^{-1} \tag{53}$$

$$\underline{P}(t \mid t-1) = \underline{A}(t)\underline{P}(t-1 \mid t-1)\underline{A}^T(t) + \underline{R}_w \tag{54}$$

$$\underline{P}(t \mid t) = \underline{P}(t \mid t-1) - \underline{K}(t)\underline{H}(t)\underline{P}(t \mid t-1) \quad (55)$$

$\underline{P}(t \mid t)$ is the covariance matrix for the state and parameter estimates at time t, given all of the information available at that time. After each update, the predictions of the model states ($MI_c^{-0.286}$, $1/\rho_c$) are again made by successive evaluations of Eqs. 45 and 46 over the next product sampling interval. These equations are then relinearized about the predictions to the forms in Eqs. 47 and 48. The entire sequence is repeated with each laboratory measurement. The EKF is tuned by changing the relative sizes of the elements in $\underline{R}_v$ and $\underline{R}_w$ as explained by MacGregor et al. (1986). EKF's are very versatile in that they can be used to update one or more parameters appearing in several model equations simultaneously and they provide updated estimates of the model states and the parameters with each new product measurement. Nevertheless, care must be taken in the formulation of EKF's. If too few parameter or disturbance states are included in $\underline{x}$, then biased estimates will be obtained due to unaccounted for nonstationary disturbances (MacGregor et al., 1986).

Recursive prediction error method

The recursive prediction error method (RPEM) is closely related to the parameter estimation part of the extended Kalman filter. Recursive prediction error schemes are generally simpler to design, tune and implement than EKF's, but they are also less flexible. RPEM's are usually formulated to update a vector of parameters, $\underline{\theta}$, in a single model equation of the form:

$$y = f[\underline{\theta}, \underline{u}(t-1), y(t-1)] \quad (56)$$

If this model is linear in the parameters, then the RPEM collapses to recursive least squares (RLS) estimation. RLS and other variants of the RPEM are commonly used in self-tuning regulator applications (Goodwin and Sin, 1984). Given the variance of the measurement error, σ_e^2, an initial vector of parameter estimates, $\underline{\hat{\theta}}(0)$, and the covariance of these estimates, Cov[$\underline{\hat{\theta}}(0)$], recursive parameter identification is accomplished by solving the following Ricatti equations:

$$\underline{\hat{\theta}}(t) = \underline{\hat{\theta}}(t-1) + \underline{L}(t-1)\epsilon(t) \quad (57)$$

$$\epsilon(t) = y_{\text{meas}}(t) - y[\underline{\theta}(t-1)] \quad (58)$$

$$\underline{L}(t-1) = \frac{\underline{Q}(t-1)\underline{Z}(t)}{\lambda + \underline{Z}^T(t)\underline{Q}(t-1)\underline{Z}(t)} \quad (59)$$

$$\underline{Q}(t) = \frac{1}{\lambda}\underline{Q}(t-1) - \frac{\underline{Q}(t-1)\underline{Z}(t)\underline{Z}^T(t)\underline{Q}(t-1)}{\lambda + \underline{Z}^T(t)\underline{Q}(t-1)\underline{Z}(t)} \quad (60)$$

$$\underline{Z}(t) = -\frac{\partial \epsilon}{\partial \underline{\theta}} = \frac{\partial y}{\partial \underline{\theta}} \quad (61)$$

$$\underline{Q}(t) = \frac{\text{Cov}[\underline{\theta}(t)]}{\sigma_e^2} \quad (62)$$

Equation 57 is similar in structure to the EKF equation (Eq. 52). $\underline{L}(t-1)$ and $\underline{K}(t)$ are both gain terms and $\epsilon(t)$ and $\underline{y}(t) - \underline{\hat{y}}(t \mid t-1)$ are prediction errors. Like $\underline{P}(t \mid t)$ in Eq. 55, $\underline{Q}(t)$ provides a measure of the covariance of the parameter estimates. The model linearization steps required for the EKF are replaced by the calculation of $\underline{Z}(t)$ whose elements are partial derivatives of the model with respect to the parameters.

To provide for time varying parameters, the RPEM has been formulated with an exponential forgetting factor, λ. Values of λ near 1 correspond to slow parameter updating whereas a smaller λ results in recent information being weighted more heavily than past data so that $\hat{\theta}$ can change quickly. A constant value of λ can result in slow parameter updating after abrupt process changes and in covariance blow-up when too much old information is discarded during periods of steady operation. To prevent these problems, Fortescue et al. (1981) have developed a variable forgetting factor algorithm which adapts λ according to the information content of the data. Their algorithm shown below results in a small λ after abrupt process changes and a λ near unity during periods when prediction errors are small:

$$\lambda(t) = 1 - \frac{1 - \underline{Z}^T(t)\underline{L}(t-1)}{\gamma}\epsilon^2(t) \quad (63)$$

Just as the rate at which parameters change is influenced by the elements of $\underline{R}_w$ in the EKF, γ is a tuning factor which influences the rate of parameter change when the RPEM is used. The latter approach, however, lacks some of the flexibility of the EKF when more than one parameter is being updated. The elements of $\underline{R}_w$ can be specified independently to influence individual parameters. Changes to γ, however, cause a similar effect in the rates of the change of all of the parameters.

Although RPE methods provide updated estimates of the model parameters whenever new observations are made, unlike the EKF, they do not simultaneously provide updated estimates of the state variables ($MI_c^{-0.286}$, $1/\rho_c$) at these instances. Obviously by updating the model parameters recursively, the prediction errors of these states are kept small over time. However, to evaluate the model equations 45 and 46 over each product sampling interval, initial conditions at the start of the interval must be given for MI_c and ρ_c. These initial conditions could be taken as the measured values at $t-1$, the predicted values at $t-1$ or some compromise between the two. A benefit of the EKF is that it automatically provides the optimal estimates as part of the update vector $\underline{\hat{x}}(t \mid t)$. To solve this problem, the RPE algorithm can be augmented with an empirical filter of the form:

$$\underline{\hat{x}}^*(t \mid t) = \underline{\hat{x}}^*(t \mid t-1) + \underline{K}^*[\underline{y}(t) - \underline{\hat{y}}(t \mid t-1)] \quad (64)$$

where $\underline{x}^* = (MI_c^{-0.286}, 1/\rho_c)^T$. This state filtering equation is of the same form as the Kalman Filter equation 52 except that $\underline{K}^*$ is assumed to be a constant matrix which is estimated from a representative record of plant data to minimize the sum of squared prediction errors. In general, for measurements with very little noise, the diagonal elements of $\underline{K}^*$ will approach unity, while for noisy measurements, these elements will be smaller.

Application of Recursive Estimation for Product Quality Inference

Before a recursive estimation scheme can be implemented, one must choose which parameters values should be adapted on-line and which should remain constant. If the recursive technique is used to fit data from a well-designed dynamic experiment, then a number of parameters can be successfully updated simultaneously. However, if the parameter estimator is applied to happenstance data, then it is better to fix most of the parameter values off-line and estimate only a few on-line. If the input to the estimator lacks sufficient information on some of the model parameters, the resulting parameter estimates will have a large covariance and will be highly correlated with the estimates of other parameters. Such correlation can be determined from the elements of $\underline{P}$ or $\underline{Q}$. While a model with poorly known and highly correlated parameters can still track the process successfully during periods of ordinary plant operation, the poor parameter estimates will initially lead to poor model predictions when a change in operating conditions occurs. Updating only a few essential parameters can help to alleviate this problem.

For the melt index and density models, the candidates for on-line updating are parameters k_1 to k_7 in Eq. 26 and p_0 to p_4 in Eq. 35. Since many different unmeasured impurities affect the instantaneous melt index, the entire $k_5[I]/[M_1]$ term is a good candidate for on-line updating. Equation 26 can be rewritten as:

$$\ln(MI) = k_7\left(\frac{1}{T}-\frac{1}{T_0}\right) + 3.5\,\ln\left(k_0 + k_1\frac{[M_2]}{[M_1]} + k_2\frac{[M_3]}{[M_1]} + k_3\frac{[H_2]}{[M_1]} + k_4\frac{[R]}{[M_1]}\right) \quad (65)$$

where $k_5[I]/[M_1]$ and k_6 have been collapsed into a single term, k_0. Updating k_0 on-line has intuitive appeal because it accounts for the effects of changing impurity levels on *MI*. Since low-level impurities have very little effect on density, there is no corresponding impurity term in Eq. 35 which should be automatically chosen for on-line estimation. If only one parameter is to be updated on-line, it must affect the model predictions, regardless of which comonomer is being used and the *MI* of the polymer being produced. For this reason, p_0 should be updated recursively. If necessary, additional parameters in either the *MI* or density models could also be chosen for on-line adaptation. In the interest of simplicity, however, it was decided that only k_0 and p_0 would be updated on-line. This choice of a single parameter for each model avoids the problem of parameter correlation in the case of non-informative data and also makes the application simple to implement and maintain. Since instantaneous and cumulative properties are identical at steady state, parameters k_1 to k_4, k_7 and p_1 to p_4 were estimated off-line using steady state plant data.

In this study, the RPEM was chosen over the EKF approach. The reasons for this choice are that the RPEM is easier to implement, has fewer parameters to specify and the potential benefits of the EKF are not realized in this simple estimation problem. To implement an EKF, the user must supply: initial estimates of the state variables and parameters, an initial covariance matrix $\underline{P}_0$, a linearized version of the model equations as shown in Eq. 47, and covariance matrices R_v and R_w. The only requirements for implementation of the RPEM are initial estimates of the parameters k_0 and p_0, initial estimates of their variances, expressions for the partial derivatives in Eq. 61, and a single tuning factor, γ, for each time varying parameter. Although the RPEM approach is recommended in this situation, the added flexibility of the EKF would be beneficial for more complex estimation problems. The potential benefits of the EKF over the RPEM include: the ability to estimate unmeasured model states, the potential for estimating several time varying parameters simultaneously while controlling the relative rate of change of each parameter, the ability to estimate parameters which appear simultaneously in several highly coupled models, and a means of optimally accounting for errors in the measured model inputs. These benefits are not realized in the estimation problem under consideration because our goal is to estimate only two time varying parameters, k_0 and p_0 which appear in two essentially uncoupled equations. Their is no requirement for the estimation of unmeasured model states nor is there any need to incorporate information on the gas composition or temperature measurement errors into the scheme. The measurement errors in these inputs are sufficiently small that they can be neglected, especially since the integration step of Eqs. 45 and 46 has an averaging effect on the individual errors. Since none of the potential benefits of the EKF are realized in this estimation problem, the two approaches should give almost identical results.

A diagram illustrating the on-line product quality inference scheme for melt index is shown in Figure 2. An analogous diagram can be drawn for density. When a new melt index measurement becomes available from the laboratory, the measurement is compared with the model prediction which corresponds to the time at which the sample was taken from the reactor. Since the sample analysis delay may be as long as one hour, a table containing past temperature and gas composition data at h minute intervals must be stored on-line. After the parameter update calculation, the current melt index estimate can be updated by applying Eq. 45 with the new value of k_0 over each h minute interval of the analysis delay, starting from the new measured value of *MI*. The prediction error used in the recursive estimation algorithm in Figure 2 is the difference

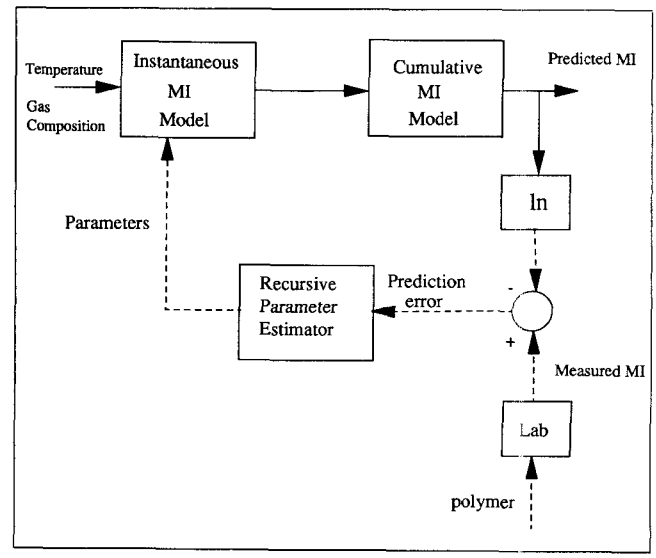

Figure 2. Melt index prediction scheme.

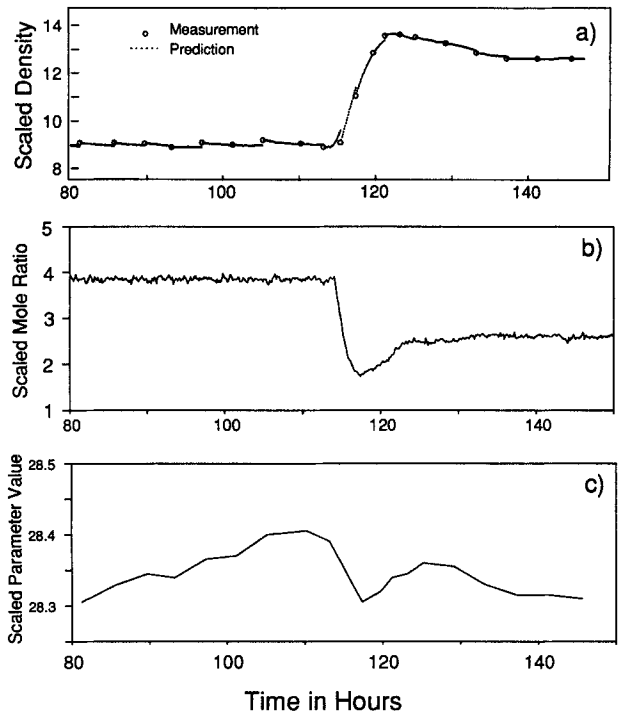

Figure 3. Recursive updating of on-line density model using industrial data.

a. Density predictions; b. gas-phase butene to ethylene mole ratio; c. parameter value, p_0.

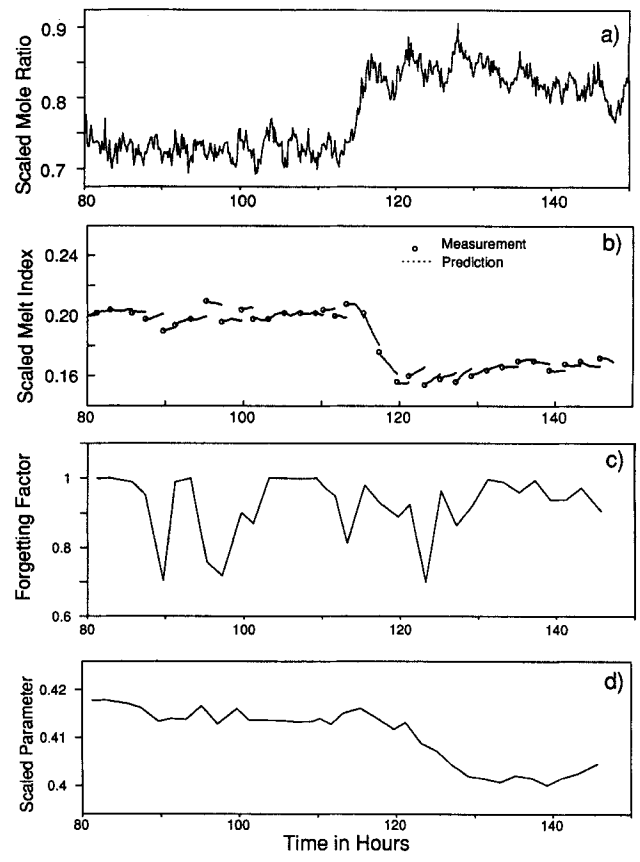

Figure 4. Recursive updating of on-line melt index model using industrial data.

a. Gas-phase hydrogen to ethylene mole ratio; b. melt index predictions; c. variable forgetting factor λ; d. parameter value, k_0.

between the logarithms of the measured and predicted *MI*'s. This transformation is used because the variance of the melt index laboratory measurement increases with the melt index level. The error variance in $\ln(MI)$, however, does not depend on the magnitude of the *MI* measurement. A constant error variance assumption is implicit in least squares type estimators, which include both the EKF and RPEM. No transformation is required for density because the measurement error variance is not level dependent. Thus, y in Eq. 56 is either $\ln(MI)$ or ρ and $\bar{\theta}$ in equation 57 is either k_0 or p_0 depending on which model is being updated. The partial derivatives required in equation 61 can be determined either numerically or analytically. The analytical expressions developed in McAuley (1991) have been used in the examples which follow. Initial parameter estimates and variances were provided from the off-line parameter identification. γ, the forgetting factor tuning parameter, was tuned to achieve the desired trade-off between information content and the speed of the parameter update.

The RPE algorithm was also augmented with the fixed gain observer Eq. 64, where the gains in $\underline{K}^*$ were estimated from some plant data to minimize the sum or squared prediction errors. Estimates of these gains were close to unity. Consequently, the measured values were used as initial conditions in integrating the prediction equations over the next step.

Results and Discussion

Typical results from the melt index and density inference scheme are shown in Figures 3 to 5. The model parameters and the γ settings required to produce these results are given in Table 1. Note that the values in Table 1 and the industrial results shown in the Figures are scaled to keep actual reactor operating conditions and model parameters proprietary. Since the reactor was operated isothermally during the period shown in the Figures, a scaled value of $\exp\{k_7(1/T_0 - 1/T)\}$ is shown in the Table rather than k_7, itself. For the conditions shown in Figures 3 to 5, $k_4[R]/[M_1]$ was very small and could be

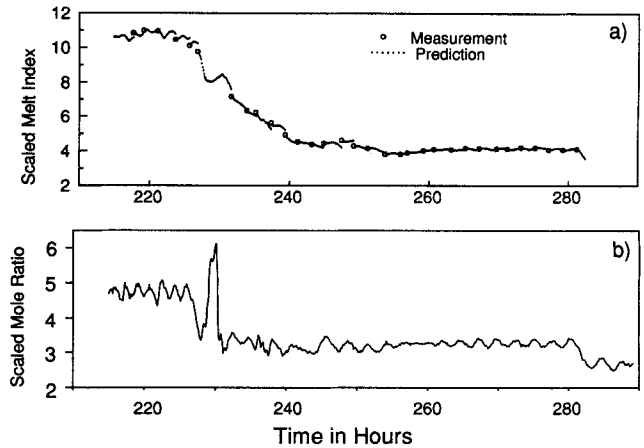

Figure 5. Predictions of on-line melt-index model during a large transition.

a. Melt index predictions; b. hydrogen to ethylene ratio.

Table 1. Scaled Parameters Required for Inference Scheme

Parameter	Scaled Value
$\exp\{k_7(1/T_0 - 1/T)\}$	0.1660
k_1	0.0726
k_3	0.3298
p_1	1.227
p_2	85.29
p_4	0.5292
γ for k_0	0.01
γ for p_0	0.25

neglected. As shown in Figure 3a, the product quality inference scheme is able to successfully track a density change from 9 to 13 scaled units. The density measurements, indicated by open circles, were performed several hours apart at irregular intervals. Any scheme used to update *MI* and ρ models on-line must account for this sporadic sampling period, as does the current RPE scheme. The small dots on the graph, which are often close enough together that they appear to form a line, represent the model predictions between the laboratory data. One dot was plotted each time the on-line gas composition measurements were made. The vertical distance between the predictions and the measurements is the density prediction error. After each laboratory measurement, the new model prediction starts at the measured value of ρ. Thereafter, Eq. 46 is used to recursively calculate each new model prediction. The density change in Figure 3a occurs in response to a reduction in the gas phase butene to ethylene ratio shown in Figure 3b. During this 70 hour time interval, the density update parameter plotted in Figure 3c, remained constant within 0.1 scaled density units, indicating that the density model was able to account for the density behavior of the industrial reactor.

The decrease in the butene to ethylene ratio at 112 hours in Figure 3b was also accompanied by an increase in the hydrogen to ethylene ratio shown in Figure 4a. Since both hydrogen and butene act as chain transfer agents, increases in their concentrations result in lower molecular weight polymer and thus in a higher melt index. Hence, the simultaneous decrease in butene and increase in hydrogen have opposite effects on *MI*, and it would be difficult to predict the resulting *MI* response without a model. As shown in Figure 4b, the on-line inference scheme was able to predict the resulting small decrease in *MI*. The prediction errors are more apparent in Figure 4b than in 3a because the ordinate scale is larger relative to the standard deviation of the laboratory measurement error. The behavior of the exponential forgetting factor, λ is shown in Figure 4c. After 120 hours, the on-line model predicts *MI* values in Figure 4b which are too high for four consecutive measurements. The RPEM algorithm responds to the first large prediction error by reducing the forgetting factor so that k_0 can be adapted quickly. As the prediction errors become smaller, λ is then allowed to increase. During this period the value of k_0 adapts to a lower level as shown in Figure 4d. This small adjustment in k_0 is required to force the model to track the process after the change in reactor operating conditions. The necessity of a change in k_0 could be attributable to any of a number of possible causes: a change in impurity levels; a drift in the gas composition analysers; a change in catalyst properties; uncertainty in the other fixed model parameters, or a slight structural inadequacy of the model. Regardless of the cause, the on-line model was able to capture the main effects of the gas composition changes and the recursive parameter estimation scheme was able to quickly adapt k_0 to eliminate any offset.

The melt index change in Figure 4b is quite small compared with the range of *MI*'s produced in the reactor. A larger transition in *MI* is shown in Figure 5. The on-line inference scheme is able to track the *MI* changes throughout this large grade transition. Even the major change which occurs between 228 and 232 hours is well-predicted by the model. The rapid swings in *MI* which occur during this period are attributable to large changes in the hydrogen to ethylene ratio which are shown in Figure 4b.

Conclusions

A methodology for on-line melt index and density prediction in an industrial fluidized bed polyethylene reactor has been presented. This scheme consists of theoretically-based models which relate melt index and density to reactor operating conditions. Adjustable parameters in the models are updated on-line by a recursive prediction error method when the results of laboratory analyses become available. It has been demonstrated that this technique is capable of successfully predicting both *MI* and ρ. These on-line predictions of melt index and density provide essential information to the polyethylene manufacturer so that a more consistent polymer can be produced.

Acknowledgment

The authors thank the Natural Science and Engineering Research Council of Canada and ESSO Chemical Canada for support of this research.

Notation

a = exponent in Eq. 1
$\underline{A}$ = coefficient matrix in linearized process model
a_2, a_3 = parameters in Eq. 27
c = subscript indicating a cumulative property
C^* = number of moles of active catalyst sites in the reactor
Ea_p = activation energy for propagation reactions
Ea_{tr} = activation energy for chain transfer in deactivation reactions
EKF = extended Kalman Filter
$\underline{G}$ = coefficient matrix in linearized process model
h = gas composition sampling interval
$\underline{H}$ = matrix relating state variables to measured variables
$[H_2]$ = gas-phase hydrogen concentration
$[I]$ = gas-phase impurity concentration
i = subscript indicating an instantaneous property
j = type of active site on the catalyst
$\underline{K}$ = Kalman gain
k_0, k_1,...k_7 = parameters in instantaneous melt index model
kf_{iH} = rate constant for chain transfer to hydrogen by an active site with terminal monomer i
kf_{im} = rate constant for chain transfer to monomer m by an active site with terminal monomer i
kf_{iR} = rate constant for chain transfer to cocatalyst by an active site with terminal monomer i
kp_{im} = propagation rate constant for the addition of monomer m to an active site with terminal monomer i
$\underline{L}$ = gain matrix in Eq. 54
M_1, M_2, M_3 = ethylene, butene and higher alpha-olefin
mf_i = mole fraction of monomer i incorporated in the polymer chains

MI = melt index
M_n = number average molecular weight
M_p = mass of polymer in the reactor
M_w = weight average molecular weight
P = covariance matrix of state and parameter estimates
$p_0, p_1, \ldots p_4$ = parameters in the instantaneous density model
P_R = polymer production rate
Q = matrix in Eq. 57
$[\bar{R}]$ = gas-phase cocatalyst concentration
R_{dI} = rate of active site deactivation by impurities
R_{fH} = rate of chain transfer to hydrogen
R_{fi} = rate of chain transfer to monomer i
R_{fR} = rate of chain transfer to cocatalyst
r_n = number average degree of polymerization
R_p = rate of propagation of living polymer chains
$RPEM$ = recursive prediction error method
R_{pi} = rate of consumption of monomer i by propagation
R_{tr} = rate of production of dead polymer chains
R_v = covariance matrix for measurement errors
R_w = covariance matrix for modeling errors
t = time
T = absolute reactor temperature
T_0 = reference temperature
u = vector of input variables in Eq. 45
v = vector of measurement errors in Eq. 46
w = vector of modeling errors in Eq. 45
w_j = weight fraction of polymer produced at site type j
x = vector of state variables
y = vector of measurements
$\bar{y}$ = model prediction
y_{meas} = measurement corresponding to model prediction
Z = vector of partial derivatives in Eq. 60

Greek Letters

ϵ = prediction error
η = viscosity of a polymer melt at low shear rates
λ = variable forgetting factor
γ = tuning parameter for variable forgetting factor
σ_e^2 = variance of prediction errors
θ = vector of parameters
ϕ_i = fraction of active sites with terminal monomer i
τ = polymer phase time constant in the fluidized bed
ρ = density

Literature Cited

Ardell, G., and B. Gumowski, "Model Prediction for Reactor Control," *Chem. Eng. Prog.*, 77 (June, 1983).

ASTM, "American Society for Testing Materials 1990 Annual Book of ASTM Standards," Vol. 8.01, Plastics (1), Philadelphia, 395, 458 (1990).

Bremner, T., D. G. Cook, and A. Rudin, "Melt Flow Index Values and Molecular Weight Distributions of Commercial Thermoplastics," *J. Appl. Polym. Sci.*, (1990).

of Olefins in a Gas-Phase Fluidized Bed," AIChE Meeting, Washington, DC (Nov. 27-Dec. 2, 1988).

Elicabe, G. E., and G. R. Meira, "Estimation and Control in Polymerization Reactors—A Review," *Polym. Eng. Sci.*, **28** (3), 121 (1988).

Ellis, M. F., T. W. Taylor, V. Gonzalez, and K. F. Jensen, "Estimation of the Molecular Weight Distribution in Batch Polymerization," *AIChE J.*, **34**, 1341 (1988).

Floyd, S., K. Y. Choi, T. W. Taylor, and W. H. Ray, "Polymerization of Olefins through Heterogeneous Catalysis: III. Polymer Particle Modelling with an Analysis of Intraparticle Heat and Mass Transfer Effects," *J. Appl. Polym. Sci.*, **32**, 2935 (1986).

Fortescue, T. R., L. S. Kershenbaum, and B. E. Ydstie, "Implementation of Self-Tuning Regulators with Variable Forgetting Factors," *Automatica*, **17**(6), 831 (1981).

Goodwin, C. G., and K. S. Sin, "Adaptive Filtering Prediction and Control," Prentice-Hall (1984).

Gagnon, L., "State Estimation and Sensor Selection for a Continuous Emulsion Polymerisation Reactor," Masters Thesis, McMaster University, Canada (1990).

Jo, J. H., and S. G. Bankhoff, "Digital Monitoring and Estimation of Polymerization Reactors," *AIChE J.*, **22**, 361 (1976).

Kozub, D. J., and J. F. MacGregor, "State Estimation and Control for Semibatch Polymerization Reactors," AIChE Meeting, San Francisco (1989).

Lennartson, B. E. V., "Combining Infrequent and Indirect Measurements by Estimation and Control," *Ind. Eng. Chem. Res.*, **28**, 1653 (1989).

Ljung, L., "System Identification—Theory for the User," Prentice-Hall Inf. and System Sci. Ser. (1987).

MacGregor, J. F., D. J. Kozub, A. Penlidis, and A. E. Hamielec, "State Estimation for Polymerization Reactors," IFAC Symp. on Dynamics and Control of Chemical Reactors and Distillation Columns, Bournemouth, UK (1986).

MacGregor, J. F., A. Penlidis, and A. E. Hamielec, "Control of Polymerization Reactors—a Review," *Polym. Proc. Eng.*, **2**, 179 (1984).

McAuley, K. B., J. F. MacGregor, and A. E. Hamielec, "A Kinetic Model for Industrial Gas Phase Ethylene Copolymerization," *AIChE J.*, **36**(6), 837 (1990).

McAuley, K. B., PhD Thesis, Dept. of Chemical Engineering, McMaster University, Canada (1991).

Richards, J. R., and P. D. Schnelle, "Perspectives on Industrial Reactor Control," *Chem. Eng. Prog.*, **84**(10), 32 (1986).

Rudin, A., "Molecular Weight Distributions," *Comprehensive Polymer Science*, Chap. 18, Vol. III, G. Allen and J. C. Bevington, eds., Pergamon Press (1989).

Sinclair, K. B., "Characteristics of Linear LPPE and Description of UCC Gas Phase Process," Process Economics Report, SRI International, Menlo Park, CA (1983).

Usami, T., Y. Gotoh, and S. Takayama, "Generation Mechanism of Short-Chain Branching Distribution in Linear Low-Density Polyethylenes," *Makromolecules*, **19**(11), 2722 (1986).

Vinodograv, G. V., and A. Ya. Malkin, "Rheology of Polymers—Viscoelasticity and Flow of Polymers," Mir Publishers, Moscow (1980).

Manuscript received Nov. 27, 1990, and revision received Apr. 4, 1991.